Ring Current Effects in Crystals. Evidence from ^{13}C Chemical Shift Tensors for Intermolecular Shielding in 4,7-Di-*t*-butylacenaphthene versus 4,7-Di-*t*-butylacenaphthylene

Zhiru Ma,[†] Merrill D. Halling,[†] Mark S. Solum,[†] James K. Harper,[†] Anita M. Orendt,[§] Julio C. Facelli,[§] Ronald J. Pugmire,[†,‡] David M. Grant,*[,†] Aaron W. Amick,[||] and Lawrence T. Scott[||]

Departments of Chemistry, Chemical Engineering, Center for High Performance Computing, University of Utah, Salt Lake City, Utah 84112, and Merket Chemistry Center, Boston College, Chestnut Hill, Massachusetts 02467-3860

Received: December 6, 2006

^{13}C chemical shift tensor data from 2D FIREMAT spectra are reported for 4,7-di-*t*-butylacenaphthene and 4,7-di-*t*-butylacenaphthylene. In addition, calculations of the chemical shielding tensors were completed at the B3LYP/6-311G** level of theory. While the experimental tensor data on 4,7-di-*t*-butylacenaphthylene are in agreement with theory and with previous data on polycyclic aromatic hydrocarbons, the experimental and theoretical data on 4,7-di-*t*-butylacenaphthene lack agreement. Instead, larger than usual differences are observed between the experimental chemical shift components and the chemical shielding tensor components calculated on a single molecule of 4,7-di-*t*-butylacenaphthene, with a root mean square (rms) error of ±7.0 ppm. The greatest deviation is concentrated in the component perpendicular to the aromatic plane, with the largest value being a 23 ppm difference between experiment and theory for the $^{13}CH_2$ carbon δ_{11} component. These differences are attributed to an intermolecular chemical shift that arises from the graphitelike, stacked arrangement of molecules found in the crystal structure of 4,7-di-*t*-butylacenaphthene. This conclusion is supported by a calculation on a trimer of molecules, which improves the agreement between experiment and theory for this component by 14 ppm and reduces the overall rms error between experiment and theory to 4.0 ppm. This intermolecular effect may be modeled with the use of nuclei independent chemical shieldings (NICS) calculations and is also observed in the isotropic ^1H chemical shift of the CH_2 protons as a 4.2 ppm difference between the solution value and the solid-state chemical shift measured via a $^{13}C-^1H$ heteronuclear correlation experiment.

Introduction

Solid-state nuclear magnetic resonance (SSNMR) has become an important tool to elucidate the structure of biological macromolecules as well as organic and inorganic materials. It is a technique routinely available in many NMR laboratories. The study of chemical shift tensors and their intermolecular effects has been an important source of information on molecular environment and electronic structure.[1] In general, the intermolecular effects on ^{13}C NMR chemical shift tensors of neutral nonpolar molecules have been found to be modest.[2] The excellent agreement observed between recent experimental shifts and calculated chemical shielding tensors[3] of PAHs (polycyclic aromatic hydrocarbons) further supports this observation. Nonetheless, extensive studies of ring current effects[4] and recent calculations of aromatic NICS[5−8] (nuclei independent chemical shieldings) indicate that the highly anisotropic molecular magnetic susceptibility that exists in PAHs may lead to strong intermolecular shielding effects for certain molecular packing arrangements in a crystal. Many PAHs crystallize in a T or herringbone type of arrangement with respect to their adjacent neighbors. This arrangement, however, is not conducive to observing intermolecular effects in the ^{13}C chemical shifts that lie along a direction perpendicular to the molecular planes.

There are, however, crystal structures of aromatic hydrocarbons (designated as γ- and β-structures) in which there are stacks of molecules lying parallel to one other.[9,10] In these cases, the ring currents can produce a large magnetic susceptibility effect on the ^{13}C chemical shifts of neighboring molecules. This type of ring current or intermolecular shift[11] has been postulated to explain the observation of three different isotropic ^1H resonances for hydrogen atoms that are expected to be magnetically equivalent in a substituted hexabenzocoronene.[12] In this case, there was no crystal structure; however, quantum calculations of the ^1H chemical shifts on a stack of molecules reproduced the trend observed experimentally.[13]

As part of our work in the development of a database of chemical shielding tensors of PAHs, we recently studied 4,7-di-*t*-butylacenaphthene, where we observed much larger than usual variations between several of the calculated and experimental ^{13}C chemical shift principal values. These divergences were well above those previously found in these types of studies, suggesting that intermolecular effects are important for this compound. The analysis of the X-ray structure of 4,7-di-*t*-butylacenaphthene revealed a packing arrangement of the molecules in the crystal with the molecular planes of neighboring molecules lined up parallel, as shown in Figure 1. This

* To whom correspondence should be addressed. Telephone: (801) 581-8854. Fax: (801) 581-8433. E-mail: grant@chem.utah.edu.
[†] Department of Chemistry, University of Utah.
[‡] Department of Chemical Engineering, University of Utah.
[§] Center for High Performance Computing, University of Utah.
[||] Boston College.

10.1021/jp068400h CCC: $37.00
Published on Web 02/22/2007

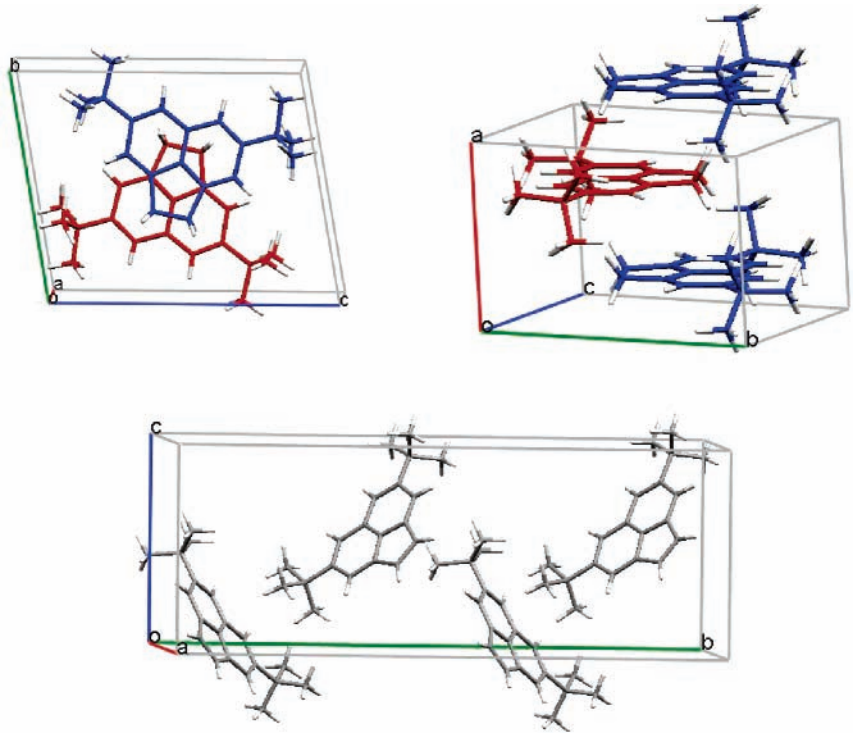

Figure 1. Crystal structures of 4,7-di-*t*-butylacenaphthene (top two views, colors are used to give specific molecular projections) and 4,7-di-*t*-butylacenaphthylene (below) showing how neighboring molecules align in the typical herringbone structure. In 4,7-di-*t*-butylacenaphthene, the CH_2 groups lie on top of and below the naphthalene ring of the neighboring molecules, maximizing the potential for ring currents or magnetic susceptibility effects reported here.

arrangement is similar to the planes in graphite but with every other molecule rotated by 180° relative to the one above and below it. These ^{13}C chemical shift principal values are different from those measured on the acenaphthene without *t*-butyl substituents, which crystallizes in the more typical herringbone structure.[2b]

In this paper, we present the measured ^{13}C chemical shift tensor principal values in triclinic 4,7-di-*t*-butylacenaphthene with coparallel planes. The related 4,7-di-*t*-butylacenaphthylene, which packs in the monoclinic and typical herringbone structure, is also shown in Figure 1. Calculations demonstrate that the observed intermolecular effects can be properly taken into account with an intermolecular shift. The effects observed experimentally are reproduced nicely by the chemical shifts calculated on the central molecule of a stack of three molecules as well as by NICS calculations using both naphthalene and 4,7-di-*t*-butylacenaphthene. This intermolecular effect is observed in a dramatic manner in the solid proton isotropic chemical shifts of the CH_2 group of 4,7-di-*t*-butylacenaphthene using a solid-state $^{13}C-^{1}H$ hetcor experiment.

The experimental data also reveal a break in symmetry caused by the crystal packing, which gives rise to additional spectral lines beyond those that one would predict on the basis of molecular symmetry in an isolated molecule. A careful examination of Figure 1 indicates that the two *t*-butyl methyl groups have nonequivalent environments in both crystal structures, and in both cases two different methyl peaks (as well as other resonance lines, vide infra) were observed. Extensive evidence of such nonsymmetrical interactions has been noted by Harper and co-workers[14,15] in comparing X-ray data obtained at the Argonne Advanced Photon Source with solid-state NMR chemical shift data that revealed additional spectral peaks because of crystal packing.

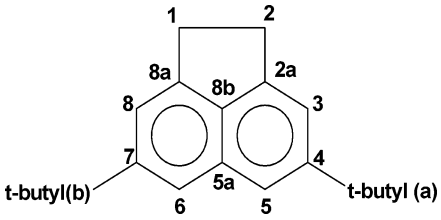

Figure 2. Numbering system for 4,7-di-*t*-butylacenaphthene (where C_1-C_2 is a single bond as shown) and for 4,7-di-*t*-butylacenaphthylene (where C_1-C_2 is a double bond).

Experimental Methods

Synthesis of 4,7-Di-*t*-butylacenaphthene and 4,7-Di-*t*-butylacenaphthylene. The syntheses of 4,7-di-*t*-butylacenaphthene and of 4,7-di-*t*-butylacenaphthylene were carried out in the laboratory of Larry Scott, and the details are presented in a recent paper.[16] The numbering system is given in Figure 2.

X-ray Structures of 4,7-Di-*t*-butylacenaphthene and 4,7-Di-*t*-butylacenaphthylene. The X-ray structures of these two molecules were determined by Scott and co-workers and can be obtained from the Cambridge Crystallographic Data Center.[17] The data for 4,7-di-*t*-butylacenaphthene and for 4,7-di-*t*-butylacenaphthylene reveal triclinic P-1 and monoclinic C*c* structures with $Z = 2$ and 4, respectively. These crystal symmetry groups both have values of $Z' = 1$, but the mirror plane symmetry through the two naphthalene central bridgehead carbons of the isolated molecule is destroyed by the lattice.

NMR Measurements. The ^{13}C NMR spectra were obtained after the fashion of data acquisition and processing methods, known as FIREMAT,[18] that are commonly used in the Utah laboratory. Cross polarization with magic angle spinning (CPMAS) spectra are referenced to tetramethylsilane (TMS) via the methyl peak of hexamethylbenzene at 17.35 ppm. A variable

contact time experiment (20 points were taken from 10 μs to 25 ms) indicated that a 7-ms contact was optimal for both structures studied. Identification of protonated and nonprotonated carbons in both structures was obtained by means of CPMAS and dipolar dephasing experiments (42 μs interrupted decoupling using pulse sequence C described by Newman[19]). The proton decoupling power was 62.5 kHz. The proton T_1 values were determined by the saturation recovery method; the values were about 160 ms for 4,7-di-*t*-butylacenaphthylene and 450 ms for 4,7-di-*t*-butylacenaphthene. A pulse delay of 2 s was used for both structures as well as a contact time of 7 ms for both the CPMAS and 2D FIREMAT experiments. The FIREMAT data were processed using the TIGER method[20] where a chemical shift sideband pattern is extracted for each model used to fit the GUIDE (isotropic spectrum without sidebands) spectrum. The fitting process and data analyses were carried out on a Sun workstation.

4,7-Di-t-butylacenaphthylene. The solid-state spectra of this compound were taken on a Chemagnetics CMX-100 spectrometer operating at a proton frequency of 100.02 MHz and a carbon frequency of 25.152 MHz using a 7.5-mm PENCIL rotor probe with a ceramic housing. The proton decoupling power was 62.5 kHz, the spinning speed was 4.1 kHz, and the proton 90° pulse was 4.2 μs.

The FIREMAT[18] experiment was run at a spinning speed of 501 Hz with 16 evolution points. The spectral width in the acquisition was 48.096 kHz and 8.016 kHz in the evolution dimension. Four thousand ninety-six data points were collected for each evolution increment and 2304 scans were acquired in each increment. The GUIDE spectrum was simulated with 13 isotropic lines representing the 20 carbons in the molecule. The carbons of the *t*-butyl groups were represented by too few sidebands for a tensor determination at the 501 Hz spinning speed. Therefore, the shift tensor principal values for these carbons were determined from a static spectrum fit with the isotropic shifts locked to those from a CPMAS spectrum.

4,7-Di-t-butylacenaphthene. The solid-state ^{13}C CPMAS and 2D FIREMAT[18] NMR experiments were performed on a Chemagnetics CMX-400 spectrometer with a ^{13}C Larmor frequency of 100.619 MHz, using a Chemagnetics 7.5-mm PENCIL rotor probe. The CPMAS experiment was run as described above with the addition of TPPM (two-pulse-phase modulation) decoupling[21] on the ^{1}H channel using a TPPM pulse of 8.6 μs and the TPPM phase of 14.0°. The spinning rate was 4 kHz and the proton 90° pulse was 4.2 μs. TPPM decoupling was also used in the 2D FIREMAT experiment, with a TPPM pulse of 8.6 μs and a TPPM phase of 36.0°.[22] The spinning rate was 850 Hz. The $\pi/2$ pulse width for ^{1}H was 4.2 μs, while the $\pi/2$ pulse width for ^{13}C was 4.3 μs. Data (i.e., 96 points) were collected during each rotor cycle. The spectral width was 81.6 kHz in the acquisition dimension and 13.6 kHz in the evolution dimension. A total of 4034 data points were collected per increment, with 16 increments in the evolution dimension. In each evolution increment, 1152 scans were acquired. The GUIDE spectrum was simulated with 11 isotropic lines representing the 20 magnetically nonequivalent carbons in the molecule.

The ^{1}H spectrum of solid 4,7-di-*t*-butylacenaphthene was obtained from an evolution dimension projection of a ^{13}C−^{1}H heteronuclear correlation experiment utilizing a wide-bore 600 MHz Varian Infinity spectrometer (^{13}C frequency 150.834 MHz). The pulse sequence proposed by van Rossum et al.[23] and Vinogradov et al.[24,25] was employed together with three Lee−Goldberg cycles per t_1 increment and an 80-μs mixing time. The other parameters included a spinning speed of 13.0 kHz, a ^{1}H 90° pulse of 2.16 μs, and spectral widths of 35.9 and 17.4 kHz in the acquisition and evolution dimensions, respectively, with TPPM decoupling in the acquisition dimension. The ^{1}H dimension was referenced to a nonspinning sample of liquid TMS in a sealed capillary at 0.0 ppm. The ^{13}C dimension was referenced to the high-frequency peak of adamantane at 38.56 ppm. All reported proton shifts were scaled by 0.577 as required for Lee−Goldburg homonuclear decoupling.[26]

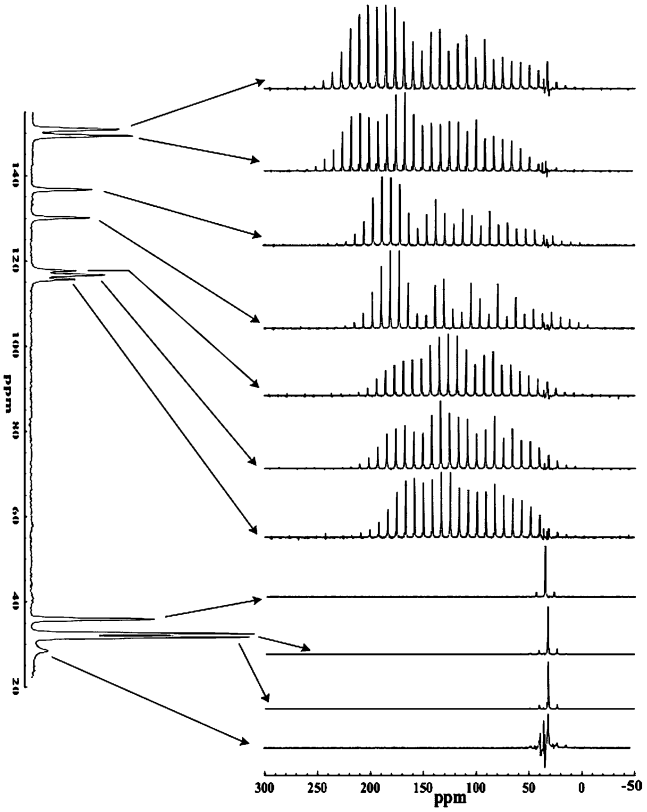

Figure 3. FIREMAT guide spectrum versus spinning sideband spectrum for 4,7-di-*t*-butylacenaphthene.

Experimental Results

The FIREMAT spectra of 4,7-di-*t*-butylacenaphthene and 4,7-di-*t*-butylacenaphthylene are shown in Figures 3 and 4, respectively. The chemical shifts from these spectra are reported in the Supplemental Tables 1 and 2, respectively. Figure 5 contains the ^{13}C−^{1}H heteronuclear (hetcor) experiment, showing an unusual ^{1}H resonance for the CH_2 hydrogens at about −0.5 ppm. The solution-phase spectrum places the proton shift of the CH_2 group at 3.65 ppm indicating a 4.2 ppm decrease in the shift of these protons in going from the solution to solid samples.

While the apparent molecular symmetry should render the peak assignments rather straightforward, such is not the case. In an individual molecule in the crystal, the bond lengths/angles are slightly different from one side of the molecule to the other, leading to each carbon being magnetically unique. These effects are compatible with the lattice symmetry of the X-ray structures of the two molecules under investigation.

In Figure 3, the pair of methyl groups ($CH_{3(a)}$ and $CH_{3(b)}$, see Supplemental Table 1) are separated by less than 1 ppm, and the shift tensor principal values also show minor differences. However, the nonprotonated carbons in the *t*-butyl groups, a and b, are accidentally degenerate with a shift of 35.9 ppm. A careful examination of the line shape suggests that a second line is present, but the solid-state resolution is not sufficient to

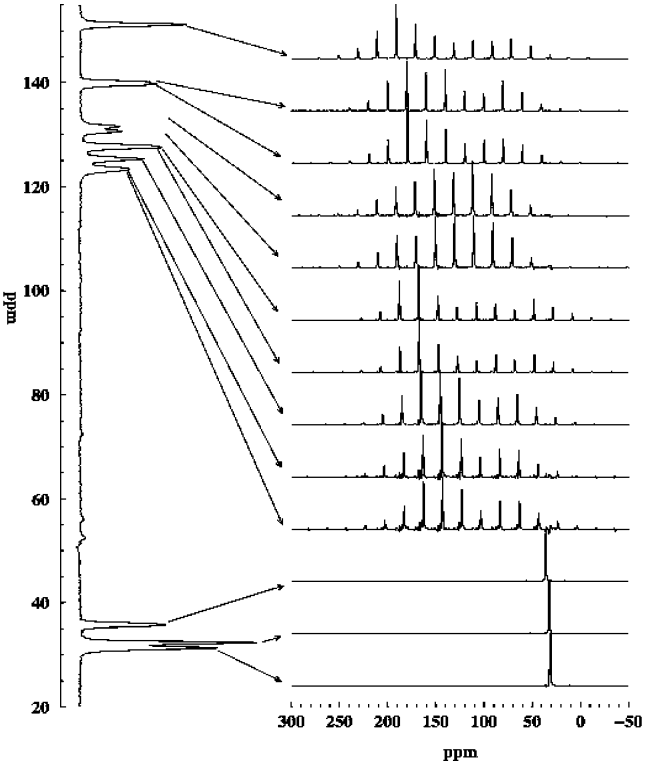

Figure 4. FIREMAT guide spectrum versus spinning sideband spectrum for 4,7-di-*t*-butylacenaphthylene.

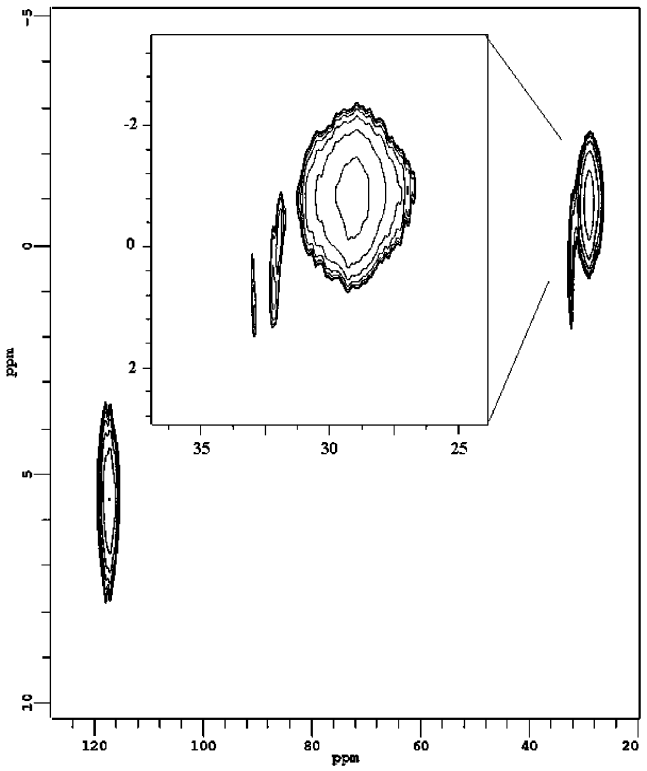

Figure 5. Solid-state $^{13}C-^{1}H$ heteronuclear correlation spectrum of 4,7-di-*t*-butylacenaphthene is shown with the ^{1}H shifts given along the ordinate axis and the ^{13}C shifts along the coordinate axis in ppm. The CH_2 group is farthest upfield.

resolve the tensors of the two carbons. The CH_2 carbons could not be completely decoupled (this is frequently observed when the decoupler frequency is centered among the proton frequencies in MAS experiments). Only one tensor could be obtained from this peak. The spectral lines for substituted carbons C_{2a} and C_{8a} were also degenerate as were the *t*-butyl substituted carbons C_4 and C_7. The shift tensors can be used to make the peak assignments for C_{5a} and C_{8b}. The C_{5a} peak is expected to be axially symmetric with a δ_{33} principal value near zero or negative. Bond strain at C_{8b}, because of attachment of a five-member ring to a naphthalene structure, produces a significant shift (16.4 ppm) in the δ_{33} principal value for the bridgehead carbon, C_{8b}, compared to that of C_{5a}, as well as a significant separation (17.3 ppm) of δ_{11} and δ_{22}.[2b] The principal values for δ_{33} for C_{5a} and C_{8b} in the parent compound, acenaphthene, are −3.1 and 13.3 ppm, respectively. The corresponding values in the *t*-butyl derivative are 2.5 and 17.8 ppm. The separation in the δ_{11} and δ_{22} principal values is 19.4 ppm at C_{8b} in the *t*-butyl derivative, whereas the principal values are degenerate in the parent compound because of axial symmetry at C_{5a}. Hence, one sees, in these data, the value of utilizing shift tensor data in making peak assignments in complicated structures. In 4,7-di-*t*-butylacenaphthene, the protonated carbons C_3, C_8 and C_5, C_6 are closely spaced but nondegenerate. Three peaks, each separated by 1 ppm, are observed with an intensity ratio of 1:2:1. This "triplet" indicates that two of the carbons are overlapped sufficiently that they cannot be resolved. The FIREMAT data for this line may be fit to two separate pairs of principal values, but the irreducible principal values of the three spectral combination of lines clearly indicate that four tensors may be extracted. Unfortunately, unambiguous assignments of the spectral data to these nonequivalent carbons are not possible. The data in Supplemental Table 1 present tentative assignments for these four carbons on the basis of the order that gave the best agreement with the theoretical calculations.

The FIREMAT data, obtained for the 4,7-di-*t*-butylacenaphthylene, are presented in Figure 4. Again, a break in the molecular symmetry is apparent from the presence of two methyl groups separated by approximately 1 ppm (also see Supplemental Table 2). The central carbons in the *t*-butyl groups are degenerate as are the substituted carbons C_4 and C_7. Two overlapping lines (the bridgehead carbons C_{5a} and C_{8b}) are discernible at 127.5 and 128.0 ppm. The assignments to C_{5a} and C_{8b} follow from the same arguments used to make the assignments of the bridgehead carbons in 4,7-di-*t*-butylacenaphthene. Carbons C_1 and C_2 are separated by 1 ppm, but the principal values are quite similar and do not provide a means for making even tentative assignments. In addition, the theoretical calculations fail to provide an assignment strategy for these carbons. Carbons C_{2a} and C_{8a} are closely spaced (shoulders are observed at 140.2 and 139.7 ppm), and they can be identified as substituted aromatic carbons on the basis of the shift principal values. The assignments for the protonated aromatic carbons C_3, C_8 and C_5, C_6 cannot be made because of their respective close proximity, 125.3 and 123 ppm. The spectral line at 125.3 ppm is due to degeneracy of two of the protonated carbons. The peak at ∼123 ppm appears to consist of two closely spaced lines separated by less than 1 ppm. The theoretical data do not provide any clues to unambiguous assignments of these peaks.

Calculations. All the chemical shielding calculations presented in this paper were performed with the GAUSSIAN03 suite of programs,[27] using the density functional theory (DFT) approach proposed by Cheeseman and co-workers,[28,29] that is, the B3LYP exchange correlation functional,[30,31] the 6-311G** basis set,[32] and the GIAO method.[33,34] The calculations in both compounds were done using the experimental X-ray structures provided by Professor Scott. Following precedence from previous investigations,[35,36] the position of the hydrogen atoms were first optimized using the GAUSSIAN03 program with the same

exchange correlation functionals and basis sets used for the shielding calculations. The experimental NMR spectra show that the three methyl groups in each of the *t*-butyl groups have the same chemical shift, indicating that these *t*-butyl groups undergo rapid rotation on the NMR time scales. Consequently, the calculated chemical shielding tensors for the three methyl groups of each *t*-butyl group were averaged in the molecular frame.[35,36] As the experimental assignments for the four overlapping protonated aromatic carbons (C_3, C_8, C_5, and C_6) of either compound could not be determined with sufficient statistical certainty, the assignments presented here are those that lead to the best agreement between the calculated and experimental values for these carbons. The calculated chemical shielding tensor components were transformed into chemical shifts using the correlation between the experimental and calculated values to determine the best intercept and slope,[36] shown in Figure 6.

For 4,7-di-*t*-butylacenaphthene, the associated intermolecular calculations use a trimer molecular model in which the two first neighbors, one above and one below, were included (the structure shown in Figure 1). The chemical shielding values from these calculations were corrected for BSSE (basis set superposition errors) using the counterpoise correction in GAUSSIAN03.[37,38] The calculations of the intermolecular electrostatic effects were carried out using the EIM (embedded ion method) as discussed in previous work.[39,40] The EIM calculations were done both with a single molecule and with the stack of three molecules imbedded in the charge array.

The intermolecular effects were also modeled using the NICS[5−8] (nucleus independent chemical shieldings) calculated at the desired positions using the same methods and basis sets. Calculations were done using both the full molecule and just the electronic structure of naphthalene as the source for NICS. The NICS results were also evaluated in an 18 × 18 × 18 regular grid with the naphthalene molecule in the center. The grid extends from 3 Å to 12.75 Å in the *z* direction (perpendicular to the naphthalene molecule) and from 4.5 Å to 12.75 Å in the *x* and *y* directions, with these distances being measured from the center of mass of the naphthalene molecule.

For 4,7-di-*t*-butylacenaphthylene, calculations were completed on an isolated molecule for the trimer shown in Figure 1 and using the EIM with a single molecule.

Discussion

In Supplemental Table 1, we present the comparison between the calculated and experimental ^{13}C chemical shift tensors in 4,7-di-*t*-butylacenaphthene, using the IUPAC numbering system as shown in Figure 2. The linear correlation between the experimental and calculated chemical shift for an isolated monomer, shown in Figure 6, has a slope of −0.9621 and an intercept of 176.9 ppm and a root mean square (rms) of 7.0 ppm. This large rms value is quite surprising when considering that values in the range of 3−5 ppm are routinely obtained for this type of calculation,[3,41,42] even when the calculation neglects the long-range intermolecular effects. In contrast, this same information is presented for 4,7-di-*t*-butylacenaphthylene in Supplemental Table 2. In this herringbone case, the rms is 4.8 ppm, as anticipated for this class of compounds; there is linear correlation between experiment and theory, which have a slope of −0.9667 and an intercept of 178.9 ppm.

Moreover, in the monomer circumstance for 4,7-di-*t*-butylacenaphthene, the largest outlier in the correlation is clearly the δ_{11} principal value of the $^{13}CH_2$ chemical shift tensor, with a difference of nearly 23 ppm between the calculated and experimental value. The calculations, as well as previous

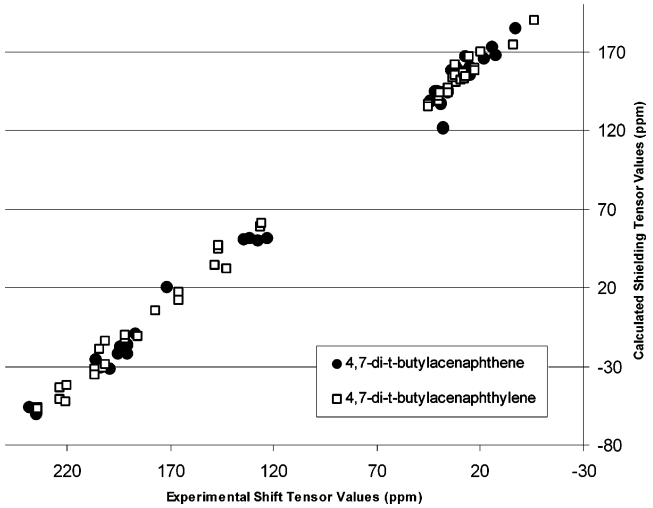

Figure 6. The correlation between the calculated ^{13}C chemical shielding and the experimental chemical shift values for 4,7-di-*t*-butylacenaphthene and for 4,7-di-*t*-butylacenaphthylene. The significant CH_2 outlier is at 120 and about 35 ppm.

precedence,[43] assign this component to be essentially perpendicular to the plane of the molecule. The large difference between the calculated and experimental values is quite surprising as the chemical shift tensor principal values of CH_2 are typically calculated with high precision.[2b,43] Moreover, it is difficult to justify the small $^{13}CH_2$ value, 37.8 ppm, of 4,7-di-*t*-butylacenaphthene when compared with the respective 48.92 and 50.46 ppm for the two methylene moieties in the parent acenaphthene compound using a previous single crystal measurement.[2b] This shift of over 11 ppm is much too large to be a remote intramolecular substituent effect of the *t*-butyl groups. In addition, calculations of this shift component for the nonsubstituted acenaphthene reproduce the experimental values quite well, that is, 48.4 and 52.8 ppm when using the RHF/DZ and 62.1 and 56.6 ppm when using the B3LYP/DZ methods, for the two CH_2 groups, respectively. The calculated value, 61.1 ppm, of this component for an isolated 4,7-di-*t*-butylacenaphthene using B3LYP/6-311G** is in good agreement with the calculated value in the parent compound. Therefore, this unexplained very large shielding effect observed in the δ_{11} component of the chemical shift tensor of the CH_2 carbon of 4,7-di-*t*-butylacenaphthene warrants further investigation. The focus of this effort was on potential intermolecular effects because of the uncommon crystal packing that may lead to this difference.

Previous work[39,40,44−48] has demonstrated that charge field models are an effective way to take into account intermolecular effects in the calculation of chemical shifts. However, in the case of 4,7-di-*t*-butylacenaphthene, the use of the EIM method[39] resulted in only a modest improvement in the rms from 7.0 to 6.2 ppm (see Supplemental Table 1). Most noticeably, no improvement is observed on the calculated valued of the δ_{11} of the CH_2 chemical shift tensor principal value. The most significant improvements provided by the EIM calculations are observed in the δ_{22} components of the bridgehead carbons C_{2a} and C_{8a}. This is quite consistent with previous observations that electrostatic effects are the largest in the shielding components perpendicular to the direction of the interaction. The δ_{22} component of the bridgehead carbons lies in the molecular plane and the proton of the CH_2 group of the neighboring molecule is only 2.6 Å above these carbons.

The lack of success of the EIM electrostatic model on 4,7-di-*t*-butylacenaphthene suggests that it is necessary to use the

TABLE 1: Comparison of the Calculated Effects on the Shielding Components, Perpendicular to the Molecular Plane, Using the Full Electron Trimer Model and the Calculated NICS at the Equivalent Positions for the Trimer, Dimer, and Naphthalene Electronic Structures[a]

		NICS		
	full electron trimer	trimer	dimer	naphthalene
CH_2 (C_1)	13.7	14.5	7.3	7.6
CH_2 (C_2)	13.5	14.6	7.4	7.2
C_{2a}	7.7	9.4	4.9	5.4
C_{8a}	8.0	9.7	5.0	4.9
C_{8b}	5.4	7.6	4.0	3.6
C_{5a}	0.9	3.2	1.7	1.0
C_3	1.0	4.5	2.4	2.9
C_8	1.8	4.8	2.5	2.3
C_7	1.2	1.5	0.8	0.6
C_4	1.0	1.3	0.7	0.8
C_5	1.1	1.2	0.7	0.4
C_6	1.4	1.3	0.7	0.3

[a] All values are in ppm.

TABLE 2: Contributions to the Intermolecular Shielding Effects to the Perpendicular Component of the Chemical Shift Tensor of the CH_2 Carbons in 4,7-Di-*t*-butylacenaphthene Calculated Using Interpolation of a Grid of NICS Values Calculated for Naphthalene[a]

first molecule above/below (*a*-axis)	7.36
second molecule above/below (*a*-axis)	0.85
third molecule above/below (*a*-axis)	0.46
first molecule along the *b*-axis	0.06
first molecule along the *c*-axis	0.01

[a] All values are in ppm.

more computationally intensive cluster method,[48,49] in which the neighboring molecules are explicitly included in the calculations. Therefore, a calculation was performed for a cluster configuration of three molecules (trimer model), adding one molecule above and one below the central molecule of interest, while preserving the geometry and interatomic distances taken from the X-ray data, along with the optimized hydrogen positions. The results of this trimer calculation are included in Supplemental Table 1. The calculated results for the trimer, with an rms value of 4.0 ppm, clearly indicate that intermolecular effects, other than those accounted for in the EIM calculation, play a very important role in the determination of the ^{13}C chemical shifts of 4,7-di-*t*-butylacenaphthene, particularly for the δ_{11} of the CH_2 carbons where the difference between experiment and theory is improved from 23 to 9 ppm. The rms between experiment and theory for the trimer system is consistent with the values obtained in many other calculations of chemical shielding in PAHs. Adding electrostatic effects by applying the EIM to the trimer has very little additional effect, leaving the rms unchanged. This indicates that the electrostatic effects originating in proximate neighbors are included implicitly in the calculations of the trimer cluster.

Aside from the change of 14 ppm in the δ_{11} of the CH_2 carbons, there are also substantial changes in several of the δ_{33} components of the aromatic carbons (the component perpendicular to the molecular plane). These changes in going from a single molecule to the trimer are summarized in Table 1 in the column headed full electron trimer. The change is the largest for carbons that are located above and below the naphthalene unit of the two neighboring molecule.

Traditionally these effects, which may also be referred to as molecular susceptibility effects,[11] have been described as "ring current effects" and have been calculated using different approximations.[4] Here, the use of NICS eliminates the need of any explicit "ring current approximation" as the NICS is calculated exactly using the quantum mechanical formulation of the chemical shifts. The calculated NICS at the position of interest is the proportionality constant between the external magnetic field and the induced field because of electron currents. Therefore, the NICS calculated at the position of interest, in this case at the position of the CH_2 of the central molecule, in the presence of neighboring molecules will give the intermolecular shielding contribution because of this effect. Using the two adjacent molecules, one above and one below, an effect of 14.5 ppm is calculated perpendicular to the molecules at the position of the CH_2 carbon. A second calculation, done by adding only one of the two neighboring molecules, resulted in a calculated effect of 7.3 ppm. The NICS calculations show a surprising additivity, indicating that the intermolecular effects are not due to indirect effects originating in the interaction of the electrons localized in the neighboring molecules but are a direct magnetic shielding effect because of the circulation of the electrons in the neighboring molecules. In Table 1, the intermolecular effects on the perpendicular shielding components of all the ring carbons in 4,7-di-*t*-butylacenaphthene calculated using the models discussed above are presented. All the effects reported in this table follow closely the trends discussed for the CH_2 carbon. In addition, the effect quickly becomes smaller as the point of interest is no longer directly above or below the aromatic portion of the structure of the neighboring 4,7-di-*t*-butylacenaphthene molecules.

Also given in Table 1 are the corresponding NICS calculated using the electronic structure of naphthalene as the source instead of the full 4,7-di-*t*-butylacenaphthene molecule. It is apparent that these NICS are quite close to those calculated for the full molecule, indicating that the intermolecular effects observed in this compound can be described entirely by the magnetic effects of field induced by the circulation of the electrons in the aromatic portion of the molecule. Therefore, further investigation of this effect may be conducted using only the aromatic portion of the molecule.

To further understand the spatial dependence of this magnetic intermolecular effect, we also calculated the NICS generated by naphthalene in a grid of points. In general, the magnetic effects exhibit the general pattern of a point dipole field, but as shown in Figure 7, there are short-range effects that do not follow the overly simple $(1 - 3\cos^2\theta)/r^3$ dependence. Therefore, it is not possible to use a point dipole model to calculate the intermolecular effects; nonetheless, it is possible to use interpolated data in the grid to calculate the magnetic shielding effects at any arbitrary position in the space relative to the source using numerical methods. This method can be used to explore the effect of second and third neighbors on the perpendicular component of the chemical shielding in the CH_2 groups of 4,7-di-*t*-butylacenaphthene. The results presented in Table 2 indicate that the intermolecular contributions are clearly dominated by the 14.7 ppm contribution from the fields generated by the first two neighboring molecules (one above and one below) along the *a* crystallographic axis. The second layer contribution is much more modest at 1.7 ppm, while the third layer contributes less than 1 ppm, for a total of 17.3 ppm. This result indicates that the remaining 9 ppm difference between experiment and theory observed in the full electron trimer calculation could be further reduced to about 6 ppm by doing a calculation of a heptamer arrangement, whenever the costs of the calculation are feasible. Finally, the contributions from the molecules in the plane of the 4,7-di-*t*-butylacenaph-

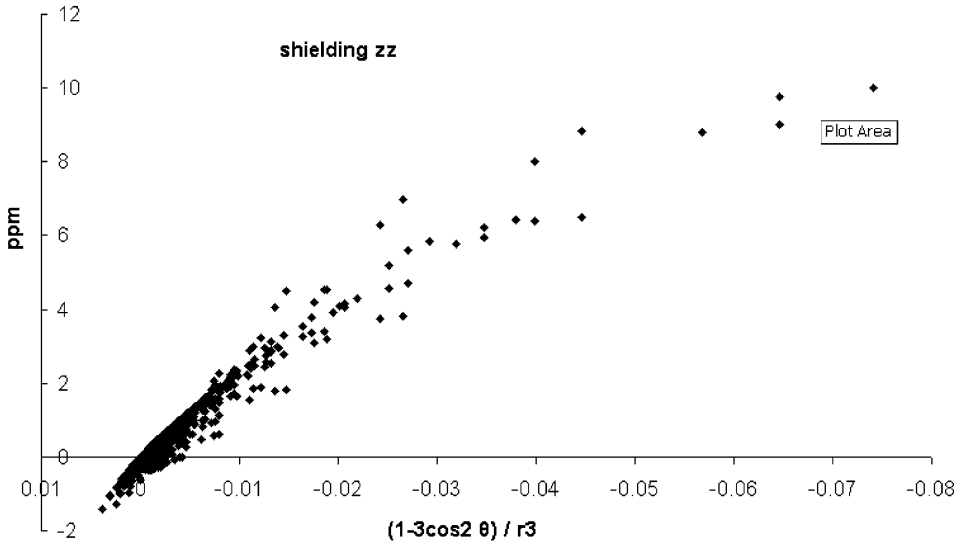

Figure 7. Distribution of the magnetic shielding effects on σ_{zz} as function of $(1-3\cos^2\theta)/r^3$.

thene molecule (along the *b* and *c* crystallographic axes) are totally negligible, as is expected because of the $\cos^2\theta$ term.

The CH_2 hydrogens are even closer to the neighboring molecules (2.6 Å) and therefore should show an even larger effect than the CH_2 carbon, as the magnitude of the effect is independent of the nucleus being measured. As this effect is only observed in the solid state, a comparison of the solution and MAS ^{1}H isotropic chemical shift was employed (via a ^{13}C−^{1}H hetcor experiment) to measure the difference because of intermolecular shielding. As noted earlier, the CH_2 hydrogen resonance in the solid state was found to be about −0.5 ppm, a difference of 4.2 ppm from the solution isotropic chemical shift of 3.65 ppm. This 4.2 ppm decrease in the isotropic ^{1}H chemical shift is huge, and the effect on the shielding solely in the direction of the NICS field would most likely be larger than this. This is an immense shift on the basis of the normal chemical shift range for protons. For comparison, the effect on the isotropic shift for the carbon of the CH_2 group is only about 2 ppm in going from solution to solid state. In the calculations, the effect on the carbon isotropic chemical shift in going from a single molecule to the trimer is less than 2 ppm because of an offset in the changes of the two other components. These changes in the other components are not necessarily due only to intermolecular effects; they can (and the EIM suggests they do) arise also from electrostatic intermolecular effects because of the presence of the neighboring molecules.

Finally, similar EIM and trimer calculation was completed on 4,7-di-*t*-butylacenaphthylene to see the effect on the agreement between experiment and theory. The EIM calculation, which uses a charge array to reproduce the crystal field lattice, does give a slight improvement of 0.1 ppm in the rms. This is indicative of cases in which intermolecular effects are negligible. The trimer calculation, on the other hand, increases the rms to 6.9 ppm.

Conclusions

In this paper, the chemical shift tensors measured via 2D FIREMAT on 4,7-di-*t*-butylacenaphthene and 4,7-di-*t*-butylacenaphthylene are reported along with a series of calculations on both compounds. The effects of crystal packing are noted in both the chemical shielding data and molecular symmetry in both the experiment and theory. In 4,7-di-*t*-butylacenaphthene, the comparison of the experimental shift tensor components with calculations on an isolated molecule shows an overall rms agreement of only 7.0 ppm, with large differences in the components that are perpendicular to the plane of the molecule. These differences are much larger in the five-member ring portion of the molecule and get smaller in regions further away from the CH_2 carbons. The largest difference is nearly 23 ppm in the δ_{11} component of the CH_2 carbon shift. Previous studies on polycyclic aromatic hydrocarbons completed in this laboratory have never shown this type of disparity. No similar disagreement between theory and experiment exists in the case of 4,7-di-*t*-butylacenaphthylene, where the rms between experiment and the single molecule calculation is 4.8 ppm.

Intermolecular interactions were explored as a potential source of this difference in 4,7-di-*t*-butylacenaphthene. The embedded ion method (EIM) was applied to this case with little success. A cluster calculation including the two nearest neighbors, one above and one below, and a central 4,7-di-*t*-butylacenaphthene, however, greatly improves the agreement, reducing the overall rms agreement from 7.0 to 4.0 ppm. Therefore, the effect would not seem to be an electrostatic intermolecular interaction but rather a magnetic effect due to the nucleus of interest being affected by the presence of additional magnetic fields from the aromatic sample.

Finally, this intermolecular effect was explored with the use of nucleus independent chemical shift calculations. The NICS calculations are less computationally extensive and can be used to calculate effects beyond the first set of nearest neighbors. The NICS calculations using only the aromatic portion of the molecule reproduce the improvement in the affected tensor components just as well as the full electron calculation on the trimer. More important, the effect is additive, allowing for summation of the effects at a position of interest from individual but different surrounding molecules. The effect is very sensitive to the intermolecular geometry; it falls off with increasing distance with an approximate $(1 - 3\cos^2\theta)/r^3$ dependence.

Acknowledgment. This work was supported by the Department of Energy, Basic Energy Sciences (DE-FG02-04ER15536 and DE-FG02-93ER14359), the National Science Foundation (EEC-0304433 and CHE-0414066), and the National Institutes of Health (Grant # 5R01 GM08521-44). The Center for High Performance Computing provided computer resources on its Arches system, which was partially funded by the National Institutes of Health (Grant # NCRR I S10 RR17214-01).

Discussions with Dr. Don Alderman on the experimental errors of the measured tensors are appreciated. Synthesis and prepublication X-ray structure data were provided by Professor Larry Scott, Merket Chemistry Center, Boston College.

Supporting Information Available: Tables comparing calculated and experimental chemical shifts in 4,7-di-*tert*-butylacenaphthene and 4,7-di-*tert*-butylacenaphthylene. This material is available free of charge via the Internet at http://pubs.acs.org.

References and Notes

(1) Representative references include (a) Yates, J. R.; Dobbins, S. E.; Pickard, C. J.; Mauri, F.; Ghi, P. Y.; Harris, R. K. *Phys. Chem. Chem. Phys.* **2005**, *7*, 1402−1407. (b) Gervais, C.; Dupree, R.; Pike, K. J.; Bonhomme, C.; Profeta, M.; Pickard, C. J.; Mauri, F. *J. Phys. Chem. A* **2005**, *109*, 6960−6969. (c) Chekmenev, E. Y.; Waddell, K. W.; Hu, J.; Gan, Z.; Wittebort, R. J.; Cross, T. A. *J. Am. Chem. Soc.* **2006**, *128*, 9849−9855. (d) Gardiennet-Doucet, C.; Assfeld, X.; Henry, B.; Tekely, P. *J. Chem. Phys. A* **2006**, *110*, 9137−9144. (e) Schoenborn, F.; Schmitt, H.; Zimmermann, H.; Haberlen, U.; Corminboeuf, C.; Grossmann, G.; Heine, T. *J. Magn. Reson.* **2005**, *175*, 52−64. (f) Harris, R. K. *Solid State Sci.* **2004**, *6*, 1025−1037. (g) Gervais, C.; Profeta, M.; Lafond, V.; Bonhomme, C.; Azais, T.; Mutin, H.; Pickard, C. J.; Mauri, F.; Babonneau, F. *Magn. Reson. Chem.* **2004**, *42*, 445−452. (h) Solis, D.; Ferraro, M. B. *Theor. Chem. Acc.* **2000**, *104*, 323−327. (i) Hansen, A. L.; Al-Hashimi, H. M. *J. Magn. Reson.* **2006**, *179*, 299−307. (j) Wong, A.; Pike, K. J.; Jenkins, R.; Clarkson, G. J.; Annpold, T.; Howes, A. P.; Crout, D. H. G.; Samoson, A.; Dupree, R.; Smith, M. E. *J. Phys. Chem. A* **2006**, *110*, 1824. (k) Barich, D. H.; Orendt, A. M.; Pugmire, R. J.; Grant, D. M. *J. Phys. Chem. A* **2000**, *104*, 8290−8295. (l) Facelli, J. C.; Hu, J. Z.; Solum, M. S.; Pugmire, R. J.; Grant, D. M. *ACS Symp. Ser.* **1999**, *732*, 162−176. (m) Facelli, J. C.; Hu, J. Z.; Orendt, A. M.; Aarif, A. M.; Pugmire, R. J.; Grant, D. M. *J. Phys. Chem.* **1994**, *98*, 12186−12190. (n) Harper, J. K.; McGeorge, G.; Grant, D. M. *Magn. Reson. Chem.* **1998**, *36*, S135−S144. (o) Harper, J. K.; McGeorge, G.; Grant, D. M. *J. Am. Chem. Soc.* **1999**, *121*, 6488−6496. (p) Harper, J. K.; Barich, D. H.; Hu, J. Z.; Strobel, G. A.; Grant, D. M. *J. Org. Chem.* **2003**, *68*, 4609−4614. (q) Harper, J. K.; Facelli, J. C.; Barich, D. H.; McGeorge, G.; Mulgrew, A. E.; Grant, D. M. *J. Am. Chem. Soc.* **2002**, *124*, 10589−10595. (r), M.; Alderman, D. W.; Grant, D. M. *J. Magn. Reson.* **2002**, *155*, 263−277.

(2) (a) Facelli, J. C.; Grant, D. M. *Nature* **1993**, *365*, 325−327. (b) Iuliucci, R. J.; Facelli, J. C.; Alderman, D. W.; Grant, D. M. *J. Am. Chem. Soc.* **1995**, *117*, 2336−2343. (c) Iuliucci, R. J.; Phung, C. G.; Facelli, J. C.; Grant, D. M. *J. Am. Chem. Soc.* **1996**, *118*, 4880−4888. (d) Iuliucci, R. J.; Phung, C. G.; Facelli, J. C.; Grant, D. M. *J. Am. Chem. Soc.* **1998**, *120*, 9305−9311.

(3) Sefzik, T.; Turco, D.; Iuliucci, R. J.; Facelli, J. C. *J. Phys. Chem. A* **2005**, *109*, 1180−1187.

(4) Lazzeretti, P. *Prog. Nucl. Magn. Reson. Spectrosc.* **2000**, *36*, 1−88.

(5) Jiao, H.; Schleyer, P. v. R. *Angew. Chem, Int. Ed. Engl.* **1996**, *35*, 2383.

(6) Schleyer, P. v. R.; Maerker, C.; Dransfeld, H.; Jiao, H.; van Eikema Hommes, N. J. R. *J. Am. Chem. Soc.* **1996**, *118*, 6317.

(7) Jemmis, E. D.; Subramanian, A. J.; Kos, P.; Schleyer, P. v. R. *J. Am. Chem. Soc.* **1997**, *119*, 9504.

(8) Facelli, J. C. *Magn. Reson. Chem.* **2006**, *44*, 401.

(9) Desiraju, G. R.; Gavezzotti, A. *J. Chem. Soc., Chem. Commun.* **1989**, 621.

(10) Desiraju, G. R.; Gavezzotti, A. *Acta Crystallogr.* **1989**, *B45*, 473.

(11) The distinction between intermolecular shielding terminology and magnetic susceptibility is more semantics than physical principles. In both cases, these terms will extend throughout the lattice and will meet the bulk criteria for separating magnetic susceptibility from chemical shielding.

(12) Brown, S. P.; Schnell. I.; Brand, J. D.; Müllen, K.; Spiess, H. W. *J. Am. Chem. Soc.* **1999**, *121*, 6712.

(13) Ochsenfeld, C.; Brown, S. P.; Schnell, I.; Gauss, J.; Spiess, H. W. *J. Am. Chem. Soc.* **2001**, *123*, 2597.

(14) Harper, J. K.; Grant, D. M.; Zhang, Y.; Lee. P. T.; Von Dreele, R. *J. Am. Chem. Soc.* **2006**, *128*, 1547.

(15) Harper, J. K.; Barich, D. H.; Heider, E. M.; Grant, D. M.; Franke, R. R.; Johnson, J. H.; Zhang, Y.; Lee. P. T.; Von Dreele, R.; Scott, B.; Williams, D.; Ansell, G. B. *Cryst. Growth Des.* **2005**, *5*, 1737.

(16) Amick, A. W.; Griswold, K. S.; Scott, L. T. *Can. J. Chem.* **2006**, *84*, 1268.

(17) CCDC 279886 and 279887 contain the supplementary crystallographic data for 4,7-di-*t*-butylacenaphthene and for 4,7-di-*t*-butylacenaphthylene, respectively. These data can be obtained free of charge from The Cambridge Crystallographic Data Centre via www.ccdc.cam.ac.uk/data_request/cif.

(18) Alderman, D. W.; McGeorge, G.; Hu, J. Z.; Pugmire, R. J.; Grant, D., M. *Mol. Phys.* **1998**, *95*, 1113.

(19) Newman, R. H. *J. Magn. Reson.* **1992**, *96*, 370.

(20) McGeorge, G.; Hu, J. Z.; Mayne, C. L.; Alderman, D. W.; Pugmire, R. J.; Grant. D. M. *J. Magn. Reson.* **1997**, *129*, 134.

(21) Bennett, A. E.; Reinstra, C. M.; Auger, M.; Lakshmi, K. V.; Griffin, R. G. *J. Chem. Phys.* **1995**, *103*, 6951.

(22) McGeorge, G.; Alderman, D. W.; Grant. D. M. *J. Magn. Reson.* **1999**, *137*, 138−143.

(23) Van Rossum, B. J.; Förster, H.; de Groot, H. J. M. *J. Magn. Reson.* **1997**, *124*, 516−519.

(24) Vinogradov, E.; Madhu, P. K.; Vega, S. *Chem. Phys. Lett.* **1999**, *314*, 443.

(25) Vinogradov, E.; Madhu, P. K.; Vega, S. *Chem. Phys. Lett.* **2002**, *354*, 193.

(26) Lee, M.; Goldburg, W. I., *Phys. Rev.* **1965**, *140*, 1261.

(27) Frisch, M. J.; Trucks, G. W.; Schlegel, H. B.; Scuseria, G. E.; Robb, M. A.; Cheeseman, J. R.; Montgomery, Jr., J. A.; Vreven, T.; Kudin, K. N.; Burant, J. C.; Millam, J. M.; Iyengar, S. S.; Tomasi, J.; Barone, V.; Mennucci, B.; Cossi, M.; Scalmani, G.; Rega, N.; Petersson, G. A.; Nakatsuji, H.; Hada, M.; Ehara, M.; Toyota, K.; Fukuda, R.; Hasegawa, J.; Ishida, M.; Nakajima, T.; Honda, Y.; Kitao, O.; Nakai, H.; Klene, M.; Li, X.; Knox, J. E.; Hratchian, H. P.; Cross, J. B.; Bakken, V.; Adamo, C.; Jaramillo, J.; Gomperts, R.; Stratmann, R. E.; Yazyev, O.; Austin, A. J.; Cammi, R.; Pomelli, C.; Ochterski, J. W.; Ayala, P. Y.; Morokuma, K.; Voth, G. A.; Salvador, P.; Dannenberg, J. J.; Zakrzewski, V. G.; Dapprich, S.; Daniels, A. D.; Strain, M. C.; Farkas, O.; Malick, D. K.; Rabuck, A. D.; Raghavachari, K.; Foresman, J. B.; Ortiz, J. V.; Cui, Q.; Baboul, A. G.; Clifford, S.; Cioslowski, J.; Stefanov, B. B.; Liu, G.; Liashenko, A.; Piskorz, P.; Komaromi, I.; Martin, R. L.; Fox, D. J.; Keith, T.; Al-Laham, M. A.; Peng, C. Y.; Nanayakkara, A.; Challacombe, M.; Gill, P. M. W.; Johnson, B.; Chen, W.; Wong, M. W.; Gonzalez, C.; Pople, J. A. *Gaussian03*, Revision C.01, Gaussian, Inc.: Wallingford, CT, 2004.

(28) Cheeseman, J. R.; Trucks, G. W.; Keith, T. A.; Frisch, M. J. *J. Chem. Phys.* **1996**, *104*, 5497−5509.

(29) Wiberg, K. B.; Hammer, J. D.; Zilm, K. W.; Cheeseman, J. R. *J. Org. Chem.* **1999**, *64*, 6394−6400.

(30) Becke, A. D. *Phys. Rev. A* **1988**, *38*, 3098−3100.

(31) Becke, A. D. *J. Chem. Phys.* **1993**, *98*, 5648−5652.

(32) Hehre, W. J.; Stewart, R. F.; Pople, J. A. *J. Chem. Phys.* **1969**, *51*, 2657−2664.

(33) Ditchfield, R. *J. Chem. Phys.* **1972**, *56*, 5688−5691.

(34) Pulay, P.; Hinton, J. F. In *Encyclopedia of NMR*; Grant, D. M., Harris, R. K., Eds.; John Wiley & Sons: London, 1996, pp 4334−4339.

(35) Grant, D. M.; Liu, F.; Iuliucci, R. J.; Phung, C. G.; Facelli, J. C.; Alderman, D. W. *Acta Crystallogr.* **1995**, *B51*, 540−546.

(36) Facelli, J. C. *Concepts Magn. Reson.* **2004**, *20A*, 42−69.

(37) Boys, S. F.; Bernardi, F. *Mol. Phys.* **1970**, *19*, 553.

(38) Simon, S.; Duran, M.; Dannenberg, J. J. *J. Chem. Phys.* **1996**, *105*, 11024.

(39) Stueber, D.; Guenneau, F. N.; Grant, D. M. *J. Chem. Phys.* **2001**, *114*, 9236−9243.

(40) Stueber, D.; Orendt, A. M.; Facelli, J. C.; Parry, R. W. Grant, D. M. *Solid State Nucl. Magn. Reson.* **2002**, *22*, 29−49.

(41) Barich, D. H.; Facelli, J. C.; Hu, J. Z.; Alderman, D. W.; Wang, W.; Pugmire, R. J.; Grant, D. M. *Magn. Reson. Chem.* **2001**, *39*, 115−121.

(42) Facelli, J. C.; Nakagawa, B. K.; Orendt, A. M.; Pugmire, R. J. *J. Phys. Chem. A* **2001**, *105*, 7468−7472.

(43) Facelli, J. C.; Orendt, A. M.; Beeler, A. J.; Solum, M. S.; Depke, G.; Malsch, K. D.; Downing, J. W.; Murthy, P. S.; Grant, D. M.; Michl, J. *J. Am. Chem. Soc.* **1985**, *107*, 6749−6754.

(44) Schneider, D. M.; Caputo, M. C.; Ferraro, M. B.; Facelli, J. C. *Int. J. Mol. Sci.* [Online] **2000**, *1*, 75−83.

(45) Ferraro, M. B.; Repetto, V.; Facelli, J. C. *Solid State Nucl. Magn. Reson.* **1998**, *10*, 185−189.

(46) Di Fiori, N.; Orendt, A. M.; Caputo, M. C.; Ferraro, M. B.; Facelli, J. C. *Magn. Reson. Chem.* **2004**, *42*, S41−S47.

(47) de Dios, A. C.; Laws, D. D.; Oldfield, E. *J. Am. Chem. Soc.* **1994**, *116*, 7784−7786.

(48) de Dios, A. C.; Oldfield, E. *Solid State Nucl. Magn. Reson.* **1996**, *6*, 101−125.

(49) Orendt, A. M.; Facelli, J. C.; Grant, D. M. *Chem. Phys. Lett.* **1999**, *302*, 499−504.